Appl. Phys. B 75, 305–310 (2002)
DOI: 10.1007/s00340-002-0982-9

Applied Physics B
Lasers and Optics

C. FISCHER
M.W. SIGRIST✉

Trace-gas sensing in the 3.3-μm region using a diode-based difference-frequency laser photoacoustic system

Swiss Federal Institute of Technology (ETH), Institute of Quantum Electronics, Hönggerberg, 8093 Zürich, Switzerland

Received: 10 April 2002/Revised version: 5 June 2002
Published online: 12 September 2002 •

ABSTRACT A compact, diode-based difference-frequency laser system combined with a photoacoustic detection scheme is presented for trace-gas sensing. It features a broad, continuous tuning range (3.2–3.7 μm), a narrow line width (154 MHz), and room-temperature operation, and thus allows numerous gas species to be measured both isolated and in mixtures of different gases. Several trace-gas species of environmental interest were detected, and gas mixtures were analysed. The detection limits are in the low-ppmV range, e.g. 1.3 ppmV for methane, 1.8 ppmV for ethane, and 1.2 ppmV for hydrogen chloride.

PACS 42.62.Fi; 42.65.Ky; 07.07.Df; 42.68.Ca

1 Introduction

The applications of trace-gas sensing comprise many different areas such as air pollution measurements in urban and rural environments, and monitoring of gas concentrations at working places, in fruit storage chambers, or in exhaled breath for medical diagnostics. For all these and for many other applications, a fast and accurate measurement of small concentrations of various gases is essential. Today, there exist several approaches to analyse gas samples with sufficient sensitivity and selectivity. We concentrate on laser spectroscopic techniques, which offer the large advantage of measurements which do not require any pretreatment and/or accumulation of the concentration of the analysed sample, unlike, for example, more conventional methods such as gas chromatography or mass spectrometry. Depending on the actual implementation of the laser-based spectrometer, different requirements need to be fulfilled. For sensitive detection, strong, i.e. fundamental, absorption lines in the mid-infrared region of the electromagnetic spectrum (3–15 μm) should preferably be chosen along with a sensitive detection scheme. In order to achieve high selectivity, e.g. for measuring different gases with the same system or for measuring isotopic ratios, the line width of the light source employed needs to be narrow, thus favouring lasers as light sources. For multi-component measurements, the tuning range of the system needs to be broad and preferably continuous. For potential applications in industry where in situ measurements are of advantage, room-temperature operation and a compact set-up are required.

The development of a system which meets as many of the above-mentioned features as possible is a challenging task. Since there is no broadly tunable narrow-band mid-infrared laser source readily available, we took advantage of nonlinear frequency conversion, in particular of difference-frequency generation (DFG). The difference frequency at ω_3 results from nonlinear mixing of two incoming photons at frequencies ω_2 and ω_1 in a nonlinear optical crystal. In order for this process to take place, both energy and momentum need to be conserved [1]. In recent years, this approach has been pursued by various research teams, mainly fostered by advances in diode and solid state laser technology, as well as in the availability of nonlinear optical crystals and periodically poled materials of good quality [2–9].

Our diode-based difference-frequency laser system combines a narrow line width, a large continuous tuning range (3.2 μm to 3.7 μm) in the so-called finger-print region where many small organic and inorganic molecules have their fundamental absorption lines, and room-temperature operation in a compact set-up.

The photoacoustic (PA) detection scheme used has the advantage that the signal measured by microphones does not exhibit a distinct intrinsic wavelength dependence, because neither optical elements with wavelength-dependent properties nor special infrared detectors are needed for a PA detection scheme. In addition, the single-pass PA cell is easy to align in the set-up. The drawback of using a PA detection scheme in combination with DFG, though, is the rather low DFG power in the micro- or milliwatt range. In photoacoustics, the measured signal scales linearly with the absorbed laser power. Higher incident power thus results in a better sensitivity.

2 Experimental set-up

The set-up employed for our measurements is depicted in Fig. 1 and has been described in detail previously [10, 11]. It basically consists of two infrared laser sources, a nonlinear crystal, and a photoacoustic cell. In contrast to the earlier set-up, the system presented here includes

✉ Fax: +41-1/633-1077, E-mail: Sigrist@iqe.phys.ethz.ch

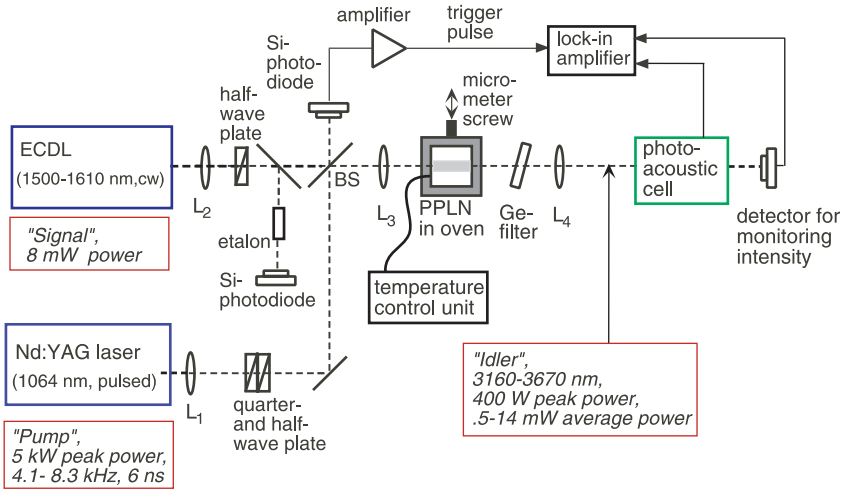

FIGURE 1 Compact set-up used for trace-gas measurements, based on a difference-frequency laser source and a photoacoustic detection scheme. L_1–L_4: lenses, BS: beam splitter

an oven with a temperature-control unit for the nonlinear periodically poled $LiNbO_3$ (PPLN) crystal.

The pump laser at frequency ω_1 is a diode-pumped Q-switched single-mode Nd:YAG laser in a nonplanar ring oscillator (NPRO) configuration (InnoLight GmbH, Hannover) [12]. It yields pulses with a peak power of about 5 kW, a pulse duration of 6 ns, and a pulse-repetition rate (PRF) of 4–8 kHz. The signal laser is a continuously tunable cw external-cavity diode laser (ECDL, EOSI, Newport) with an average power of about 5 mW. The wavelength range accessible with the ECDL lies between 1500 nm and 1600 nm. The two laser beams are focussed onto the nonlinear crystal where the DFG process takes place via quasi-phase matching. Due to energy conservation, the wavelength of the generated light can easily be calculated from the wavelengths of the signal and pump lasers. The nonlinear optical crystal employed for the measurements is an AR-coated PPLN crystal with eight different grating periods between 28.5 µm and 29.9 µm and a length of 50 mm (Crystal Technologies, Palo Alto).

The tuning of the generated difference-frequency wavelength is carried out by varying two parameters. On the one hand, the wavelength of the signal laser is changed in order to reach different wavelengths. Energy conservation determines which wavelength will be generated if the quasi-phase-matching condition is fulfilled, i.e. if the crystal period length is appropriately chosen. On the other hand, the period length is adjusted by selecting the right grating period of the PPLN crystal (out of eight periods as given by the crystal manufacturer) and by heating the crystal to the right temperature. Although the temperature acceptance bandwidth of $LiNbO_3$ is rather large (17 °C), the crystal still needs to be heated to roughly the optimised temperature. Figure 2 shows the grating periods for most efficient frequency conversion as a function of temperature for five of the eight grating periods. The other three grating periods of the PPLN are not used for DFG due to the limited ECDL tuning range.

Only by selecting the right grating and by varying both parameters – temperature and signal wavelength – is efficient phase matching over a large wavelength range possible.

The resulting DFG radiation has a tuning range between 3.2 µm and 3.7 µm and a line width of 154 MHz at an average power of about 2 mW [13]. The line width resulting from

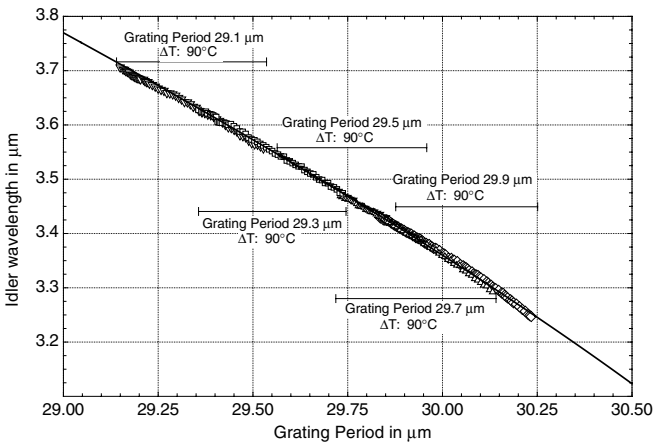

FIGURE 2 Tuning characteristics for five different grating periods of the PPLN crystal. ΔT is the temperature-tuning range (35–125 °C) of the PPLN for the overlapping wavelength ranges shown. The *solid line* represents the calculated tuning curve

a pure DFG process is given by the convolution of the line widths of the two lasers. As the ECDL is very narrowband (< 100 kHz), the line width of the DFG beam is essentially given by the line width of the Nd:YAG laser. The DFG line width has been determined directly from spectroscopic gas absorption measurements on formaldehyde (CH_2O) at reduced total pressure [13]. However, there are always two additional processes present when generating the difference frequency: optical parametric generation (OPG) and amplification (OPA). DFG is a process where two incoming waves interact in a nonlinear material. If the phase-matching condition is met, frequency conversion will take place. The intensity of the generated light scales with the intensities of the two incoming beams. The wavelength of the generated light is given by energy conservation, which results in the narrow line width of the DFG beam. OPA, in contrast, is a process where three incoming beams interact in a nonlinear material. Two of the beams are amplified at the cost of the third beam. This process can only take place if either the intensity of the incoming pump beam (the laser beam with the highest frequency) is high enough to generate a photon at the signal and at the idler wavelengths, which can then in turn be amplified,

i.e. if the pump beam is intense enough to undergo an OPG process, or if there already exist photons at the signal and idler wavelengths, e.g. from DFG or some other source like quantum noise. As OPA is an amplification process, its intensity scales exponentially with the input electric field. Thus, for high pump intensities the OPA process will become dominant over the DFG process. The wavelength and thus the line width of the generated beam in an OPG/OPA process depend on the various acceptance bandwidths for nonlinear processes; in the case of PPLN, mainly on the temperature acceptance bandwidth (17 °C) and thus results in a large line width. In order to keep the narrow line width of 154 MHz, the average DFG laser power is usually kept at or below about 2 mW. Owing to the large temperature acceptance bandwidth, the DFG line width is in this case not influenced by temperature fluctuations of up to a few °C. A higher power up to 14 mW has been generated, yet with a broadened line width of 195 GHz at 14-mW output power (i.e. about three orders of magnitude larger) due to optical parametric processes simultaneously taking place. If the selectivity of the system is not an important issue, e.g. in a gas mixture with only a few components with well-separated absorption lines, higher output powers can be taken advantage of to enhance the sensitivity of the PA measurements.

The DFG beam is focussed into a single-pass resonant photoacoustic cell. The PA cell is equipped with four miniature electret microphones (Sennheiser) and has especially been constructed for the laser system [11]. The first longitudinal resonance frequency of the PA cell occurs at 5.7 kHz and coincides with the pulse-repetition frequency of the Nd:YAG pump laser. The jitter resulting from the passive Q-switching of the Nd:YAG laser is $< 1\%$. As the resonance curve of the PA cell is rather broad (FWHM = 1.38 kHz resulting in the low Q-factor of 4), this jitter does not have a major impact on the sensitivity of the PA cell. The PRF of the laser can in addition be stabilised by fine tuning the diode current of the Nd:YAG laser to actually meet the resonance frequency of 5.7 kHz of the PA cell during the whole measuring period. The compact cell has two buffer volumes housing the gas inlets and outlets, which are placed at pressure nodes of the first longitudinal acoustic resonance. These means substantially suppress noise originating from the gas flow whenever measurements are performed on flowing gas.

The cell is sealed off with two BaF_2 windows at Brewster angle again placed at pressure nodes of the acoustic resonance to reduce the window heating signals. Furthermore, the air-tight seal allows measurements at lowered pressure (down to about 200 mbar) where the absorption features become more distinct. At even lower pressure (below about 200 mbar), the responsivity of the microphones drops significantly as studies with similar electret microphones have shown previously [14].

The measurements are carried out fully automated controlled by a computer. Thus, sensing over long periods of time is feasible.

3 Measurements and results

We employed the system to monitor several trace gases at different wavelengths and under different experimental conditions. The system can be used both for measuring single gases at low concentrations, and for analysing mixtures of different gases. Synthetic air (79.5% nitrogen and 20.5% oxygen) was used as buffer gas for the measurements presented here, which were all carried out at room temperature and at different total pressures. The use of synthetic air ensures that the pressure broadening is the same as in ambient air.

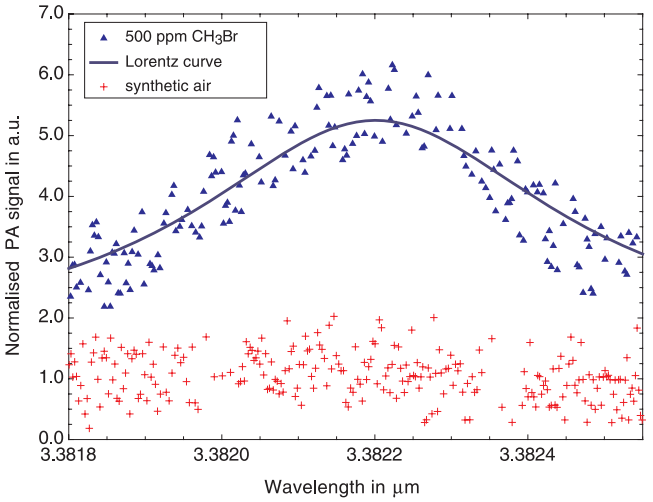

FIGURE 3 Measurement of methyl bromide buffered in synthetic air at room temperature and atmospheric pressure. The *solid curve* represents a Lorentz curve of the pressure-broadened absorption line. The background signal of synthetic air is represented by the data points at the *bottom*

Figure 3 shows a recorded spectrum of methyl bromide (CH_3Br) around 3.382 μm. Methyl bromide is widely used in agriculture and plays a key role in atmospheric chemistry [15]. Like many additional spectra taken of CH_3Br, as well as of other gases, this spectrum serves as a reference spectrum which allows us to analyse multi-component gas samples. Since there is no HITRAN data [16] available for CH_3Br, and since the NIST database [17] only offers a resolution of 0.1 cm^{-1}, i.e. much lower than the resolution achieved with our system (0.005 cm^{-1}), the measured data has been compared to a Lorentz curve. The current detection limit for CH_3Br (ν_1 band) is 250 ppmV at a signal-to-noise ratio (SNR) of 3. An averaging time of 2 s per data point was chosen, resulting in a total measurement time of about 20 min. The strong scattering of the PA signal can be attributed to large power fluctuations and the short averaging time used for these preliminary measurements. If time resolution is not an issue, longer averaging times could result in improved detection limits, especially at low DFG power levels where the optical parametric processes can be neglected.

Figure 4 shows the recorded spectrum of a two-component gas sample containing 9 ppmV ethane (ν_7 band) and 10 ppmV methane (ν_3 band) buffered in synthetic air. Methane is known as one of the major greenhouse gases while ethane is considered as an important compound to study the effect of stress on living tissue, particularly on plants [18]. The measurement example clearly demonstrates the advantage of the large and continuous tuning range as strong absorption lines of the two gases can be used for detection, which considerably improves the detection limits of both gases. The insets of the figure indicate that, despite the large tuning range, the resolution of each recorded spectrum is good and by far sufficient for multi-

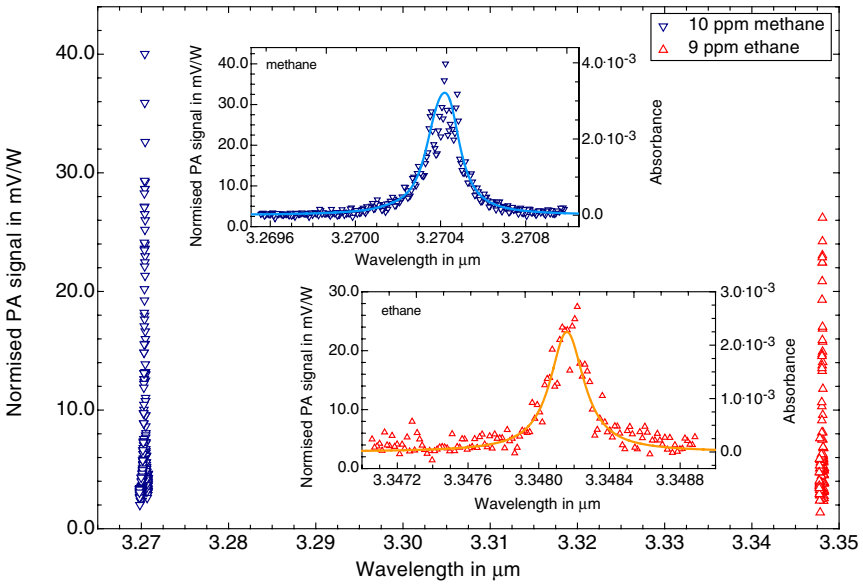

FIGURE 4 Combined spectrum of 9 ppmV ethane and 10 ppmV methane diluted in synthetic air, recorded at room temperature and 1-bar total pressure. The *solid lines* in the *insets* represent the calculated spectra using the HITRAN database (*right-hand scale*). The *data points* represent the normalised PA signal amplitudes (*left-hand scale*)

component measurements. The figure shows the measured normalised PA signals in comparison to the calculated spectra using the HITRAN database.

The PA signal fluctuations at the peak of the absorption lines are larger than at the base. A possible explanation is the fact that the DFG power for these two measurements was in the range of 3 mW, indicating that OPG/OPA processes enlarged the line width of the DFG radiation. The noise level was determined from the baseline signal. The fluctuations of the PA signal at peak absorption could be reduced by operating the system at lower incident DFG (OPG/OPA) power as shown in Fig. 5. This observation implies that a reduced power results in an improved SNR of the generated PA signal. It should be noted, though, that this statement is a particular feature of the DFG system used here. The measurement of these two gases at the spectral resolution shown in the two insets takes about 40 min each. If the resolution is lowered, e.g. by taking fewer data points for each species or by reducing the averaging time for each data point, the recording time can significantly be reduced. Between the measurements, only the temperature of the nonlinear crystal needs to be changed slightly. As mentioned above, the nonlinear quasi-phase-matching process responsible for the frequency conversion is characterised by a rather large temperature acceptance bandwidth of about 17 °C. In this case, this is an advantage since the temperature only needs to be roughly adjusted to the optimum temperature. From these measurements, the detection limits of methane and ethane at the wavelengths indicated in the figure can be calculated, yielding 1.3 ppm (SNR = 3) for methane and 1.8 ppm (SNR = 3) for ethane.

Figure 5 shows the detailed measurement of 90 ppmV methane in a mixture of 500 ppmV methyl bromide and 9 ppmV ethane diluted in synthetic air carried out at room temperature and at two different total pressures (1 bar and 300 mbar). The measurement of methane was not carried out at the maximum absorption strength, but in a section of the electromagnetic spectrum where there is no interference from the other gases present in the cell.

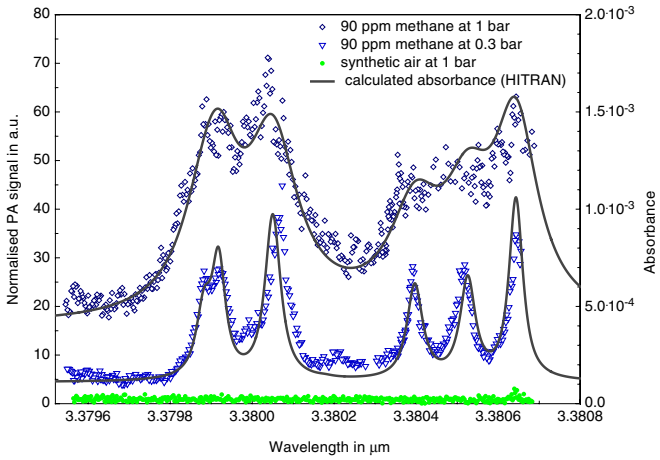

FIGURE 5 Detailed measurement of 90 ppmV methane in a mixture with 500 ppmV methyl bromide and 9 ppmV ethane buffered in synthetic air at room temperature and two different total pressures. The *solid lines* represent the calculated spectra according to the HITRAN database (*right-hand scale*). The *data points* represent the normalised PA signal amplitudes (*left-hand scale*). The background signal for synthetic air at a pressure of 1 bar is plotted at the *bottom*

The obtained data agrees well with the calculated data from the HITRAN database. The figure again demonstrates the advantage of a narrow line width allowing highly resolved measurements. Especially, at a lowered pressure where the pressure broadening is reduced, the individual absorption lines of methane become well visible (300 mbar in the case of Fig. 5). The PA signal decrease with decreasing gas pressure is in qualitative agreement with the HITRAN data calculated for the two pressures. The decrease of the PA signal is, however, somewhat stronger than predicted, which is caused by a slightly reduced microphone responsivity at lower pressure. This aspect, though, has been investigated in more detail previously with another type of electret microphone and different experimental conditions [14]. In that study, single laser pulses and a nonresonant PA cell were employed. In addition, the laser fluence was high enough to saturate the absorption.

The reduction of the microphone responsivity in the above-cited study was particularly pronounced for pressures below 300 mbar, but may be different for the microphones used in the present study.

The discrepancy between the recorded and the calculated spectra at 3.3802 μm, which is more pronounced at lower pressure, most probably results from a water absorption line. Other deviations, e.g. around 3.380 μm and 3.305 μm, might result from the presence of methyl bromide. The elevated floor can also be explained by the presence of methyl bromide.

A further aspect concerns the noise level of the recorded signal, which is smaller at lower pressure. A similar effect was found in another study with a quantum-cascade laser with similar output power as the DFG source used here [19]. A possible explanation of this observation is that at lower pressure the coupling of ambient noise outside the cell into the cell is reduced owing to the reduction of the acoustic impedance difference between the outside and the inside of the cell. Although both these observations – with the DFG source and the quantum-cascade laser – seem to indicate that it could be advantageous to operate a PA system at lower pressure to improve the noise level (and possibly the signal-to-noise ratio), further investigations are required before general conclusions can be drawn on its implications for PA gas measurements. It has also to be kept in mind that a reduction of the gas pressure can only be favourable for continuously tunable laser sources unless the emission spectrum of a line-tunable source coincides exactly with the peak absorption of the sample analysed.

From the measurements (shown in Figs. 3–5 and others), the detection limits of several gases could be determined as listed in Table 1 at a signal-to-noise ratio of 3. In addition, the theoretically calculated detection limits of other gases accessible with the system are given based on their absorption strength. Compared to long-path absorption measurements using DFG systems where detection limits down to ppbV levels have been demonstrated (see e.g. [7]), the detection limits achieved here are obviously higher. It should be noted, however, that the PA detection scheme offers several advantageous features as discussed below, notably easy alignment and small cell volume (120 cm^3 in this study). In addition, many applications, e.g. working place surveillance, do not require ppbV detection sensitivity.

Table 1 gives the name of the gas and the chemical formula as well as the absorbance, the measured or calculated detection limit at the wavelength specified, and the maximum permissible working place concentration (MAK). The absorbance is the value given in the HITRAN database for a gas concentration of 100 ppmV at room temperature and one bar total pressure for an absorption path length of 1 m at the wavelength specified. The maximum permissible working place concentrations are taken from [20]. The comparison of the detection limits and the MAK data implies that certain substances can easily be monitored at working places, especially methane and ethane while, for other substances, the detection limit needs to be improved. As mentioned above, the signal in a PA detection scheme is proportional to the incident laser power, to the number of absorbing molecules and their absorption cross section, and to the Q-factor of the gas cell in the case of an acoustic resonance. The absorption cross section is an intrinsic parameter of the gas species analysed. The absorption strength and hence the absorbed power can be optimised by choosing an appropriate wavelength of the light source. The Q-factor of the cell and the incident laser power can both be tailored. Increasing the laser power would involve either increasing the power of the incident laser beams or, preferably, better adjustment of the nonlinear crystal. The maximum theoretically achievable average power for pure DFG radiation (neglecting all absorption and reflection losses) is approximately 3 mW, which is close to the measured DFG power, indicating that at the current incident laser powers other nonlinear processes are either already present or just about to become important. As mentioned above, higher signal and pump power would improve the idler power, yet at the cost of a broader line width due to increased power originating from OPG/OPA processes. Thus, it might be difficult to further enhance the DFG power by readjusting the nonlinear crystal. Hence, the most promising approach to improve the detection limits lies in the design of a PA cell with a higher Q-factor, in multi-pass configuration, and/or insertion of more microphones.

When increasing the Q-factor of the PA cell, care has to be taken of the cited frequency fluctuations of the Q-switched Nd:YAG pump laser. A 20-times higher Q-factor (of 80), for

Gas	Formula	Absorbance[a]	Wavelength	Detection limit	MAK[b]
Ethane	C_2H_6	0.383	3.348 μm	1.8 ppmV	10000 ppmV
Methane	CH_4	0.181	3.381 μm	3.8 ppmV	10000 ppmV
		0.493	3.270 μm	1.3 ppmV	
Methyl bromide	CH_3Br		3.382 μm	∼ 250 ppmV	5 ppmV
Methyl chloride	CH_3Cl	0.062	3.372 μm	11 ppmV	50 ppmV
Hydrogen chloride	HCl	0.613	3.375 μm	1.2 ppmV	5 ppmV
Carbonyl sulfide	OCS	0.018	3.410 μm	40 ppmV	
Nitrogen dioxide	NO_2	0.046	3.428 μm	15 ppmV	3 ppmV
Ozone	O_3	0.0027	3.460 μm	250 ppmV	0.1 ppmV
Formaldehyde	H_2CO	0.239	3.574 μm	3 ppmV	0.5 ppmV

[a] Absorbance $A = \log(1/T)$; T = transmission for a concentration of 100 ppm diluted in synthetic air (20.5% oxygen, 79.5% nitrogen) at room temperature and 1-bar total pressure, calculated for a path length of 1 m and a concentration of 100 ppmV

[b] MAK = maximum permissible working place concentration

TABLE 1 Detection limits of the gases measured and for some selected gases accessible with the system

example, would result in a resonance width of about 70 Hz (FWHM) and hence the jitter of the Nd:YAG laser of less than 1% (about 50 Hz) would result in PA signal fluctuations of almost 50%.

A probably more promising approach would be a multi-pass configuration as successfully realised in another study [21]. With a 36-fold increase of the path length a 19-fold PA signal enhancement was achieved. This type of signal enhancement, though, is at the cost of the compact cell design. In addition, a multi-pass configuration requires highly reflecting mirrors. An even more straightforward approach might thus be a resonant cell equipped with more microphones. A compact nonresonant 80-microphone cell has been presented in [22]. It could be demonstrated that the PA signal scales with the number of microphones (N) whereas the signal-to-noise ratio scales with $N^{1/2}$. Even in combination with a resonant cell, a substantial signal enhancement can be expected. An improvement in the detection limits by a factor of 10 to 100 thus appears feasible with a carefully designed compact PA cell.

4 Conclusion

A laser spectroscopic scheme for trace-gas sensing based on difference-frequency generation and photoacoustic detection has successfully been applied to trace-gas detection and multi-component analysis with detection limits in the low-ppmV range. The broad and continuous tuning range allows multi-component measurements. In a gas mixture, each species can be analysed at a wavelength where the absorption features are very distinct and unique. On the one hand, the large tuning range enables higher sensitivity. On the other hand, it also extends the dynamic range by the possibility to monitor one and the same species at different wavelengths exhibiting different absorption cross sections. In addition, the narrow line width of the laser source helps distinguishing between different components of the gas mixture even if the absorption lines of the gas under investigation appear at almost the same positions. Thus, the stated detection limits are not only valid for interference-free measurement conditions, but in most cases also apply to multi-component mixtures because the DFG wavelength can be tuned to an appropriate wavelength. The narrow line width also allows high-resolution measurements, e.g. at lowered pressure only limited by the accuracy at which the wavelength of the two incident laser beams can be measured (≤ 1 pm).

The photoacoustic detection scheme has the advantage that the alignment of the cell is fairly easy, unlike multi-pass cells. Furthermore, the transverse beam profile is less critical. In addition, no optics exhibiting wavelength-dependent transmission and/or reflection characteristics is used, which is important for measurements over a large tuning range. This also reduces contamination problems encountered in field experiments. The same PA cell can also be employed for other wavelength ranges, which is not generally possible for other detection schemes such as cavity ring-down. Finally, no cooled detectors are required as the signal is recorded by microphones.

The drawback of the system is that the laser power of the DFG signal is rather low for photoacoustics, thus limiting the sensitivity of the system. Improvements of the PA cell design and an enhancement of the DFG laser power by further optimising the adjustment of the nonlinear crystal or employment of a nonlinear material with higher conversion efficiency should result in considerably lower detection limits.

ACKNOWLEDGEMENTS The authors would like to thank Prof. Q. Yu (Dalian University of Technology, P.R. China) for his valuable assistance.

REFERENCES

1 R.L. Byer, R.L. Herbst: Parametric Oscillation and Mixing. In: *Nonlinear Infrared Generation* (Top. Appl. Phys. **16**), ed. by Y.R. Shen (Springer, Berlin, Heidelberg, New York 1977) Chap. 3
2 D. Richter, D.K. Lancaster, R.F. Curl, W. Neu, F.K. Tittel: Appl. Phys. B **67**, 347 (1998)
3 M. Seiter, M.W. Sigrist: Appl. Opt. **38**, 4691 (1999)
4 V. Petrov, C. Rempel, K.-P. Stolberg, W. Schade: Appl. Opt. **37**, 4925 (1998)
5 D. Mazzotti, P. De Natale, G. Giusfredi, C. Fort, J.A. Mitchell, L.W. Hollberg: Appl. Phys. B **70**, 747 (2000)
6 K. Fradkin-Kashi, A. Arie, P. Urenski, G. Rosenman: Opt. Lett. **25**, 743 (2000)
7 D.G. Lancaster, A. Fried, B. Wert, B. Henry, F.K. Tittel: Appl. Opt. **39**, 4436 (2000)
8 D. Mazzotti, G. Giusfredi, P. Concio, P. De Natale: Opt. Lasers Eng. **37**, 143 (2002)
9 B. Sumpf, K. Kelz, M. Nägele, H.-D. Kronfeldt: Appl. Phys. B **64**, 521 (1997)
10 M. Seiter, M.W. Sigrist: Infrared Phys. Technol. **41**, 259 (2000)
11 C. Fischer, Q. Yu, M. Seiter, M.W. Sigrist: Opt. Lett. **26**, 1609 (2001)
12 I. Freitag, A. Tünnermann, H. Welling: Opt. Lett. **22**, 706 (1997)
13 M. Seiter: Novel Pulsed Difference-Frequency Laser Sources for Compact Mid-IR Trace-Gas Sensing. In: *Series in Quantum Electronics*, Vol. 14, ed. by H. Baltes, P. Günter, U. Keller, F.K. Kneubühl, W. Lukosz, H. Melchior, M.W. Sigrist (Hartung Gorre, Konstanz 1999)
14 I.G. Calasso, M.W. Sigrist: Rev. Sci. Instrum. **70**, 4569 (1999)
15 J.H. Butler, J.M. Rodriguez: Methyl Bromide in the Atmosphere. In: *The Methyl Bromide Issue*, ed. by C. Bell, N. Price, B. Chakrabarti (Wiley, London 1996)
16 L.S. Rothman, C.P. Rinsland, A. Goldman, S.T. Massie, D.P. Edwards, J.-M. Flaud, A. Perrin, C. Camy-Peyret, V. Dana, J.-Y. Mandin, J. Schroeder, A. McCann, R.R. Gamache, R.B. Wattson, K. Yoshino, K.V. Chance, K.W. Jucks, L.R. Brown, V. Nemtchinov, P. Varanasi: J. Quantum Spectrosc. Radiat. Transfer **48**, 665 (1996)
17 NIST: Quantitative Infrared Database, Standard Reference Database 79, http://www.nist.gov/srd/nist79.htm
18 R.R. Wise, A.W. Nylor: Plant Physiol. **83**, 272 (1987)
19 D. Hofstetter, M. Beck, J. Faist, M. Nägele, M.W. Sigrist: Opt. Lett. **26**, 887 (2001)
20 SUVA: in *Grenzwerte am Arbeitsplatz* (Swiss Government 1999)
21 M. Naegele, M.W. Sigrist: Appl. Phys. B **70**, 895 (2000)
22 M.W. Sigrist, A. Bohren, I.G. Calasso, M. Naegele, A. Romann, M. Seiter: *13th Symp. Sch. High-Resolution Molecular Spectroscopy* [Proc. SPIE **4063**, 17 (2000)]